

Lysozyme/tripolyphosphate complex coacervates: Properties, curcumin encapsulation and antibacterial activity

Maximiliano L. Agazzi^{a,*}, M. Fernanda Paletti Rovey^b, Eugenia Apuzzo^c, Santiago E. Herrera^d, Mariana B. Spesia^a, M.de las Mercedes Oliva^b, Omar Azzaroni^{c,**}

^a Instituto para el Desarrollo Agroindustrial y de la Salud (IDAS), (UNRC, CONICET), Ruta Nacional 36 KM 601, 5800, Río Cuarto, Argentina

^b Instituto de Biotecnología Ambiental y Salud (INBIAS), (UNRC, CONICET), Ruta Nacional 36 KM 601, 5800, Río Cuarto, Argentina

^c Instituto de Investigaciones Físicoquímicas Teóricas y Aplicadas (INIFTA), (UNLP, CONICET), Sucursal 4, Casilla de Correo 16, 1900, La Plata, Argentina

^d Departamento de Química Inorgánica, Analítica y Química Física, INQUIMAE, CONICET, Facultad de Ciencias Exactas y Naturales, Ciudad Universitaria, Pabellón 2, Buenos Aires, C1428EHA, Argentina

ARTICLE INFO

Keywords:

Coacervation
Lysozyme
Tripolyphosphate
Curcumin
Encapsulation
Antibacterial activity

ABSTRACT

Complex coacervates based on the combination of two oppositely charged biopolymers have been proposed as encapsulating and protective platforms for bioactive agents in food science. Lysozyme, an enzymatic protein used as a natural food preservative, was combined with other macromolecules (proteins and polysaccharides) to generate coacervate formulations. In this study, the design of coacervate-like structures based on lysozyme was extended through their combination with multivalent tripolyphosphate anion, a non-macromolecular food additive. It was observed that direct mixing led to the formation of complex coacervates under certain ranges of pH, ionic strength, and component concentrations. Coacervates presented a suitable capacity to encapsulate poorly water-soluble curcumin. More interestingly, coacervates improved the chemical stability (under long-term storage and light irradiation) and antibacterial activity of curcumin. Therefore, these single macromolecule coacervates could be exploited as an active carrier platform for encapsulation in food applications.

1. Introduction

The combination of oppositely charged polyelectrolytes in an aqueous medium results in an associative phase separation in which a polyelectrolyte-poor phase and a polyelectrolyte-rich phase are formed (Blocher & Perry, 2017; Friedowitz et al., 2021; Sing & Perry, 2020). Depending on the macromolecules structures and the experimental parameters, the polyelectrolyte-rich phase can display characteristics of a liquid (complex coacervate), a solid, or a combination of both configurations (Chen et al., 2021; Kurtz et al., 2019; Meng et al., 2020).

Coacervation has been exploited for the design of soft formulations with applications in different technological fields, including food technology, personal care products, and medicine (Warnakulasuriya & Nickerson, 2018; Zhou et al., 2020). In food science, complex coacervates have been proposed dually: 1) as structuring and stabilizing materials in emulsions and 2) as carrier to encapsulate, protect and controlled release of bioactive agents (e.g., vitamins, antioxidants, antimicrobial, oil components and probiotics) (Cortés-Morales et al.,

2021; Devi et al., 2017; Moschakis & Biliaderis, 2017; Shaddel et al., 2018; J. Zheng et al., 2020).

Although polyelectrolytes are diverse and highly abundant in nature, food science relies primarily on proteins and polysaccharides due to their biocompatibility, high availability and nutritional properties (Eghbal & Choudhary, 2018; Santos et al., 2018, 2021). These biopolymers can present positive or negative net charges depending on the pH selected. Lysozyme (LYS) is a globular protein that is widely distributed in nature and it is used as a food natural preservative due to its bacteriostatic activity (Khorshidian et al., 2022; Wu et al., 2019). By its exceptional cationic character in a wide range of pH ($pI \approx 11.16$ with 12 charges per protein when fully ionized) (Kuehner et al., 1999), LYS is suitable to act as cationic building block in the preparation of polyelectrolyte complexes. In this sense, a long series of protein/polysaccharide complexes have been reported based on the combination of LYS with pectin, hyaluronic acid, gum Arabic, cellulose, carrageenan, among others (Amara et al., 2017; Antonov & Zhuravleva, 2020; Z. Li et al., 2015; Xu et al., 2014; W. Zhang et al., 2020). Furthermore,

* Corresponding author.

** Corresponding author.

E-mail addresses: magazzi@exa.unrc.edu.ar (M.L. Agazzi), omarazzaroni@quimica.unlp.edu.ar (O. Azzaroni).

heteroprotein complexes were prepared from the assembly of LYS with other proteins, including gelatin B, soy proteins (β -conglycinin), whey proteins (β -casein, albumin bovine serum, α -lactalbumin, β -lactoglobulin and lactoferrin), and egg proteins (ovalbumin) (Anema & de Kruijff, 2013; Antonov et al., 2017; Croguennec et al., 2017; Monteiro et al., 2016).

Recently, single-polyelectrolyte complexes have been prepared from assembly between a polyelectrolyte and an oppositely charged small ion (Agazzi et al., 2019; Herrera et al., 2019, 2020). Here, the small ion can be of any nature and even can come from the protonation or deprotonation of organic molecules like carboxylic acids and amines. Like polyelectrolyte complexes, polyelectrolyte-multivalent ion complexes can be obtained both as solid precipitates and liquid coacervates. As a constraint, for phase separation to occur, the charge of the small ion must be high enough (typically $|z| \geq 2$) (Herrera et al., 2023). Frequently, polyamines (i.e., polyallylamine, polyethylenimine, polylysine and chitosan) have been shown to form complexes with multivalent anions such as phosphates, citrates, and sulphates, among others (Agazzi et al., 2020a; Agazzi et al., 2020; Kumari et al., 2019; Lawrence & Lapitsky, 2015). Lapitsky et al. reported several studies using polyallylamine/tripolyphosphate (TPP) coacervates to encapsulate different molecules, including therapeutics and biocides agents (Alam et al., 2020; 2021, de Silva et al., 2018). Previously, it was shown that polyphosphates (including TPP) have the ability to modify the solubility of LYS and induce associative phase separation of proteins (Bye & Curtis, 2019; Bye et al., 2013). Because TPP is a cheap multivalent molecule widely used as food additive (Lampila, 2013), its combination with LYS could allow the preparation of food-grade coacervates for encapsulation of bioactive molecules.

One of the most attractive nutraceutical and functional agents in food industry is curcumin (CUR), a bioactive natural compound obtained from the root of *Curcuma longa*. CUR is used as coloring and flavoring agents in food processing (Rafiee et al., 2019). Recently, it has emerged as a promising plant-based preservative due to its antioxidant and antimicrobial properties (Gómez-Estaca et al., 2017; Zorofchian Moghadamtoosi et al., 2014). However, CUR is highly hydrophobic and unstable in the presence of different environmental conditions such as light irradiation (B. Zheng & McClements, 2020). To improve its solubility and stability, different encapsulation strategies have been applied such as emulsions, biopolymer nanoparticles, vesicles, among others (Rafiee et al., 2019; B. Zheng & McClements, 2020). Also, coacervates have been exploited as CUR encapsulating platforms (Mirmohammad Meiguni et al., 2022; Shahgholian & Rajabzadeh, 2016). Particularly, LYS-based coacervates with conglycinin and cellulose showed ability to encapsulate and protect CUR (Z. Li et al., 2015; J. Zheng et al., 2022).

Given the previously described background, this work explores for the first time the physicochemical and encapsulation properties of single-biomacromolecule complex coacervates based on the combination of two food additives such as LYS and TPP. We study the formation and physical-chemical properties of LYS/TPP complexes varying the components concentrations, pH and ionic strength. Then, the encapsulation and protection (under long-term storage and light irradiation) of CUR was evaluated. Finally, the antibacterial activity of complexes and CUR-loaded complexes was analyzed. The results indicate that this new type of complex coacervate present attractive and promising properties for microencapsulation of functional food additives.

2. Materials and methods

2.1. Materials

The lyophilized Lysozyme powder (L6876, protein $\geq 90\%$) from chicken egg white, sodium tripolyphosphate (STPP) and curcumin (CUR) from *Curcuma longa* (Turmeric) were purchased from Sigma-Aldrich (St. Louis, MO, USA). All chemicals were used without further purification.

2.2. Preparation of LYS/TPP complex coacervates

LYS/TPP complex coacervates were formed by mixing equal volumes of aqueous solutions of LYS (10 mg mL⁻¹, pH 4) and TPP (100 mM, pH 8.5) in deionized water. The pH of both solutions was adjusted with aliquots of HCl or NaOH solutions (0.1 M). The final pH after mixing was around 9. The colloidal solution was kept at room temperature until complete phase separation. To assess the range of concentrations where phase separation occurs, complex formation was evaluated by mixing different final concentrations of LYS (0.5, 1, 2.5, 5, and 10 mg mL⁻¹) and TPP (0.1, 0.25, 0.5, 1, 2.5, 5, 10, 15, 20, 25, 40, 50 mM).

2.3. Zeta potential measurements

Zeta potential measurements were carried out with a ZetaSizer Nano (ZEN3600, Malvern, U.K.) at 20 °C using DTS1060 disposable cuvettes. Particle Zeta potential was determined from the electrophoretic mobility by Laser Doppler Velocimetry using a general-purpose analysis method with 100 runs for each sample.

2.4. Turbidity measurements

The transmittance (T) of samples were recorded at 580 nm using a 1 cm pathlength glass cuvettes by a Shimadzu UV-2401PC spectrophotometer (SHIMADZU Co., Japan). Milli-Q water was used to calibrate for 100% transmittance. The turbidity was calculated as follows:

$$\text{Turbidity} = -\ln T$$

2.5. Protein crosslinking yield

The previously prepared LYS/TPP complexes were centrifuged at 9000 × g for 5 min. The protein content that remained in the supernatant was determined by measuring the absorption of LYS at 280 nm and using a calibration curve in water (Fig. S1a).

The protein crosslinking yield was calculated as follows:

$$\text{Protein crosslinking yield (\%)} = \left(1 - \frac{\text{LYZ in supernatant}}{\text{Total LYZ content}} \right) \times 100\%$$

2.6. Microscopic observation

Microscopic observations were made with an inverted microscope (BIM500FL, Bioimager, ON, Canada). Samples were first prepared in 1.5 mL microcentrifuge tubes and allowed to settle for 1 h for the phase separation to fully form. Then, 20 μ L of coacervate mixture were placed on a glass slide. Images were collected using a 100 × magnification objective with oil immersion (Carl Zeiss CP ACHROMAT 40 × ; Carl Zeiss CP ACHROMAT 100 × , NA = 1.25).

2.7. CUR encapsulation efficiency

CUR-containing complexes were prepared added CUR to LYS solution from a stock solution (8 mg mL⁻¹) in absolute ethanol under magnetically stirred conditions. After that, TPP was added to the mix to activate the complexation. For encapsulation measurements, LYS/CUR/TPP complexes were centrifuged at 9000 × g for 5 min. CUR remaining in the supernatant was determined by measuring the absorption at 425 nm and using a calibration curve in ethanol/10% water (Fig. S1b). Next, the encapsulation efficiency was calculated as follows:

$$\text{Encapsulation efficiency (\%)} = \left(1 - \frac{\text{CUR in supernatant}}{\text{Total CUR content}} \right) \times 100\%$$

2.8. CUR degradation experiments

Degradation of CUR by storage over time and light irradiation were performed for the LYS/CUR/TPP complexes and control solutions of LYS/CUR, TPP/CUR and CUR free. In all cases, the following component concentrations were used: 2.5 mg mL⁻¹ LYS, 2.5 mM TPP and 250 µg mL⁻¹ CUR. The remaining CUR at the end of the experiment (see next section) was determined following a protocol previously (J. Zheng et al., 2022). For the complexes LYS/CUR/TPP, the samples were vortexed after adding absolute ethanol (five times the initial volume) to extract the remaining CUR. Mixtures were then centrifuged at 9000×g for 5 min to remove the LYS/TPP complexes without CUR. The content of CUR in the remaining supernatant was determined by UV-Vis absorption at 425 nm using a calibration curve of CUR in absolute ethanol/10% water. The preservation of CUR over time was calculated as follows:

$$\text{CUR preservation percentage (\%)} = \frac{\text{Remaining CUR}}{\text{Initial CUR content}} \times 100\%$$

2.8.1. Photochemical degradation

LYS/CUR/TPP complexes and aqueous solutions at pH 9 of LYS/CUR, TPP/CUR and CUR free were irradiated at two different intervals of times (2.5 and 5 h) with visible light. As a source of irradiation, a Novamat 130 AF projector (Braun Photo Technik, Nürnberg, Germany) equipped with a 150 W halogen lamp was used. A 2.5 cm wide water-filled cuvette was used as a filter to absorb the heat from the lamp.

2.8.2. Storage stability

The free CUR, TPP/CUR, LYS/CUR, and LYS/CUR/TPP complexes at pH 9 were stored at 4 °C in dark for different intervals of time (1, 5, 10, 15 and 20 days).

2.9. Lysozyme enzyme activity

The enzymatic activity of LYS was analyzed using the well-established method of inducing cellular lysis in *Micrococcus luteus* (Yang et al., 2017). To measure the effect of ionic complexation on LYS lytic activity, the optical density at 600 nm (OD_{600nm}) was measured in *Micrococcus luteus* culture in the presence of samples of LYS (5 mg mL⁻¹), LYS/TPP complexes (5 mg mL⁻¹ LYS, 2.5 mM TPP) and disassembled LYS/TPP complexes. In the latter, the complex coacervates were allowed to settle for 2 h and then disassembled by reducing the pH to 6, obtaining uncomplexed LYS and TPP. Culture of *M. luteus* was prepared in Mueller-Hinton (M-H) broth (Britania, Buenos Aires, Argentina) and incubated for 24 h at 37 °C. Then, a 1/10 dilution (~10⁶ CFU mL⁻¹) was made and 2 ml aliquots of the culture were divided into test tubes. Samples were added to each tube at a final concentration of 5 mg mL⁻¹ LYS and 2.5 mM TPP. Then they were incubated for 90 min at 37 °C in an orbital shaker (Ferca). Finally, the OD_{600nm} for each sample was measured in a spectrophotometer (Spectrum, SP 2000). The growth control was *M. luteus* grown in M-H broth.

2.10. Curcumin antibacterial activity

The antimicrobial activity of LYS/CUR/TPP complexes (2.5 mg mL⁻¹, 250 µg mL⁻¹ CUR and 2.5 mM TPP) in water/5% ethanol was evaluated on three Gram positive strains (*Staphylococcus aureus* ATCC 25923, *S. aureus* DM1 and *S. aureus* DM2) employing a modification of the Kirby-Bauer methodology (Clinical and Laboratory Standards Institute, 2012). Briefly, Petri plates with Mueller Hinton agar (MHA) were seeded with 100 µL of each standardized microbial suspension (0.5 McFarland scale) and spread with Drigalsky spatula. Then, drops (20 µL) with different concentrations of LYS/CUR/TPP complex coacervates were placed on previously seeded MHA plates and incubated at 37 °C for 18–24 h. Besides, LYS free (2.5 mg mL⁻¹ in water/5% ethanol), TPP free (2.5 mM in water/5% ethanol), CUR (50, 250 and 500 µg mL⁻¹ in

water/5% ethanol), and LYS/TPP (2.5 mg mL⁻¹ LYS and 2.5 mM TPP) controls were studied. In addition, the activity of complexes loaded with CUR was measured after 20 days post-preparation and compared with CUR in water/5% ethanol after 20 days of storage. The inhibitory activity was evaluated by measuring the diameter of the clear zone (growth inhibition halo) around the drop. The diameter of the growth inhibition halo constitutes a measure of the susceptibility of the bacterium to each sample applied. In all cases, the experiments were carried out in triplicate.

The antibacterial activity was also evaluated by monitoring the growth curves of the *S. aureus* ATCC 25923 strain in the presence of LYS/CUR/TPP complexes and controls (LYS, LYS/TPP complexes and CUR). In all cases the concentrations of LYS, TPP and CUR were 2.5 mg mL⁻¹, 2.5 mM and 250 µg mL⁻¹, respectively. Bacteria were grown aerobically on a rotator shaker (100 rpm) at 37 °C in MH broth overnight. Then, a portion (20 µL) of this culture was transferred to 20 mL of fresh MH broth medium. This suspension was homogenized, and 1 mL aliquots of microbial stock solution were placed in culture tubes with 1 mL of each sample. Each tube was incubated at 37 °C and the cell culture growth was monitored by turbidity at 700 nm every 60 min. Moreover, growth control (GC) was performed to know the normal development of the microorganism and then be able to compare with the obtained curves after the different treatments. GC consisted of 1 mL of microbial suspension and 1 mL sterile water. All measurements were performed in triplicate.

3. Results and discussion

3.1. Preparation and characterization of LYS/TPP complex coacervates

Complexation of LYS with TPP was qualitatively studied by direct mixing of components in aqueous solutions and under constant stirring, varying different parameters such as initial pHs (pH⁰) and relative concentrations. In the process, we detected a dramatic increase in turbidity, especially when working with TPP at pH⁰ = 8.5 and LYS at pH⁰ = 4. Note that, in this scenario, TPP displays 5 net charges per molecule (pKa₁ = 1; pKa₂ = 2.2; pKa₃ = 2.3; pKa₄ = 5.7; pKa₅ = 8.5) and LYS present a cationic character (pI = 11.16). The increase in turbidity is indicative of the formation of complexes between LYS and TPP, driven by the formation of ion pairs between positively charged residues in LYS and TPP anions. In most of cases, the final pH of the solution was ~9, which is indicative of the releasing of OH⁻ during the complexation process. This could be indicative of the forced (or cooperative) ionization over uncharged LYS amine moieties (Petrov et al., 2003).

A simplified representation of the phase separation process is shown in Fig. 1. Immediately after complexation, the solution was highly turbid (colloidal dispersion of LYS/TPP complexes). After a few minutes, two distinct macroscopic phases were spontaneously separated: one translucent at the top and one opaque at the bottom (see pictures in Fig. 1).

To explore the concentration regions space where phase separation is produced, LYS and TPP were combined at different concentrations and the samples were allowed to stand for 1 h. Fig. 2a shows the concentration zone where phase separation occurred (colored dots). As can be observed in the plot, below [LYS] = 1 mg mL⁻¹ the system is unable to form complexes, independently on the concentration of TPP. This sets a minimum concentration of LYS molecules needed to produce complexation with TPP. For all concentrations of LYS, we also found that there is a minimum concentration of TPP where an appreciable phase separation occurs. Furthermore, we also observed that, for a given concentration of LYS, there is a second phase boundary at which the system resolubilizes (a maximum TPP concentration). In this case, the maximum TPP concentration was found to increase linearly with the concentration of LYS (see second transition line in the phase diagram). As so, at fixed LYS concentration, the system first condenses into 2 phases (first threshold) and then transitions back into a 1-phase system (second threshold) with increasing TPP concentration. This phenomenon is known as re-entrant

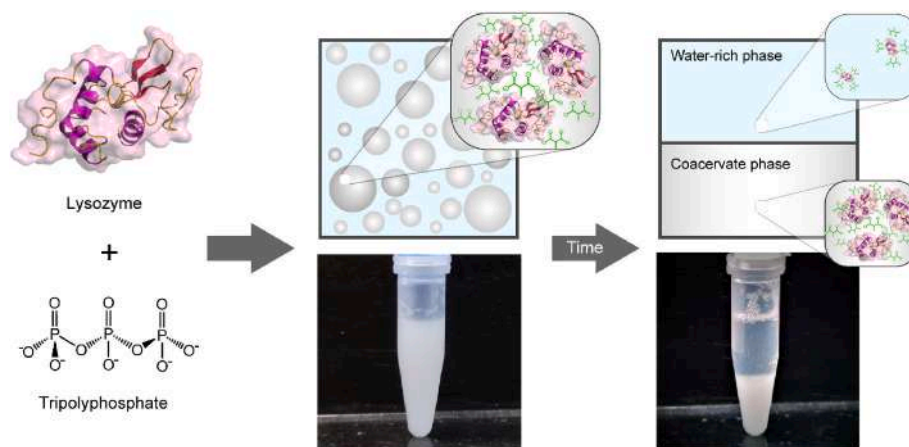


Fig. 1. Simplified representation of phase separation process activated by the LYS/TPP complexation.

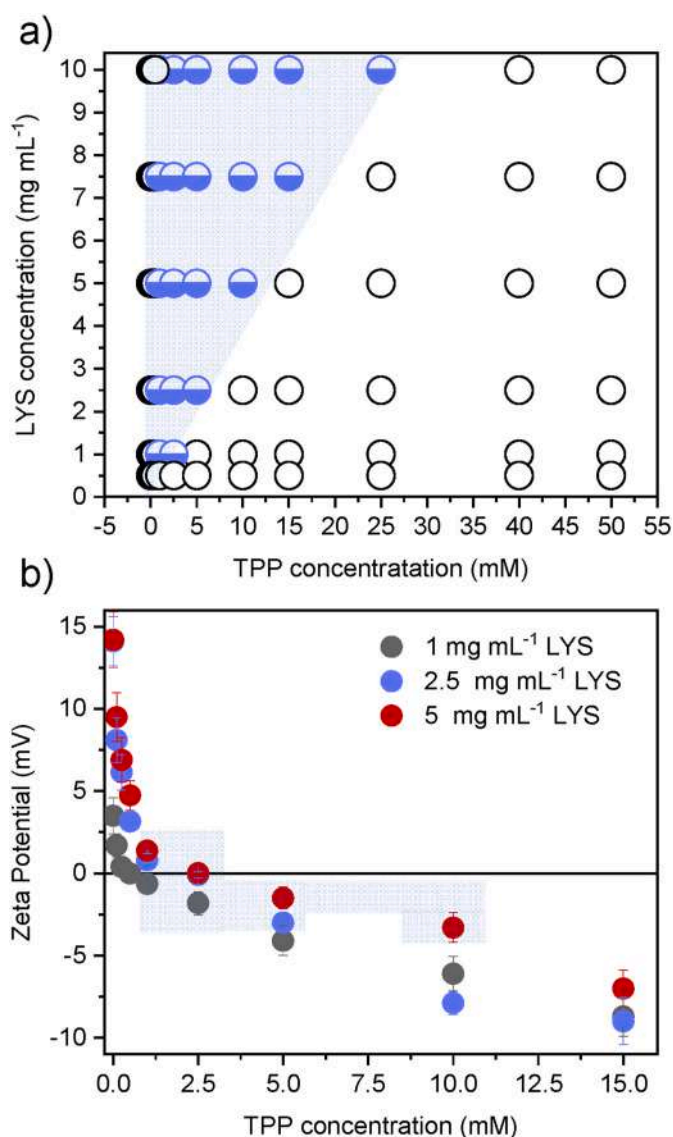


Fig. 2. a) Region of LYS and TPP concentrations where the phase separation occurs (colored circles indicate the presence of two phases) b) Zeta potential as a function of TPP concentration at three LYS concentrations (1, 2.5 and 5 mg mL⁻¹). The phase separation zone is colored in blue in both plots.

condensation. The first TPP threshold is given when the minimum of multivalent ions that are necessary to overcome repulsive interactions between positively charged proteins is reached. On the other hand, the second transition threshold can either be attributed to overcharging of the protein by the addition of an excess of multivalent ions or to charge-screening effects (Bye & Curtis, 2019).

Next, we studied the phase separation behavior by registering the ξ -potential at three LYS concentrations (1, 2.5 and 5 mg mL⁻¹) and variable TPP concentration (Fig. 2b). As it was expected, the phase separation region is coincident with ξ -potentials close to neutrality ($|\xi$ -potential| < 5 mV). As TPP concentration increases, the maximum complexation takes place when the charges on the protein are fully compensated by TPP anions. In these conditions (ξ -potential \approx 0 mV), complexes formed present a poor colloidal stability, which facilitates the formation of two macroscopic phases rapidly.

The phase separation process also was explored by turbidity and protein crosslinking efficiency (protein crosslinking yield) measurements. We observed that turbidity increased as TPP was added until reaching a maximum in the phase separation region (Fig. 3a). Then, with further TPP addition, turbidity decreased until practically total transparency was reached, indicating protein re-solubilization. In addition, turbidity within the phase separation region was consistently higher for increasing concentrations of LYS. For example, for LYS at 1, 2.5 and 5 mg mL⁻¹ (at TPP concentration of 2.5 mM) the turbidity values were 1.37, 3.0 and 4.6, respectively.

The content of protein within the complex phase (protein crosslinking yield) is nearly a mirror image of the turbidity curve, with the highest values within the phase separation region (Fig. 3b). Furthermore, the crosslinking yield increased for increasing LYS concentrations. For example, at 1, 2.5 and 5 mg mL⁻¹ of LYS (at TPP concentration of 2.5 mM) the maximum crosslinking yields were 37%, 73%, and 81%, respectively. After determining the concentration region where the phase separation occurred, we proceeded to study the properties of the aggregates under these conditions.

The condensed phase can exist in different physical states: coacervates (liquid-liquid phase separation), precipitates (solid-liquid phase separation), or a combination of both configurations (Comert & Dubin, 2017; Comert et al., 2016). The final state of the aggregate will depend on a balance of weak interactions (hydrophilicity, hydrogen bonding, electrostatics) which vary depending on various parameters as concentrations, ionization degree, polyelectrolyte's backbone structure, ionic strength, and pH. These parameters influence the strength of the attractive force that determines the dominance of each configuration (Thongkaew et al., 2015; J. Zheng et al., 2022b). Typically, bright-field microscopy and phase-contrast microscopy are used as the main techniques to distinguish liquid-liquid phase separation from solid-liquid phase separation (Devi et al., 2017; Marciel et al., 2017). When liquid

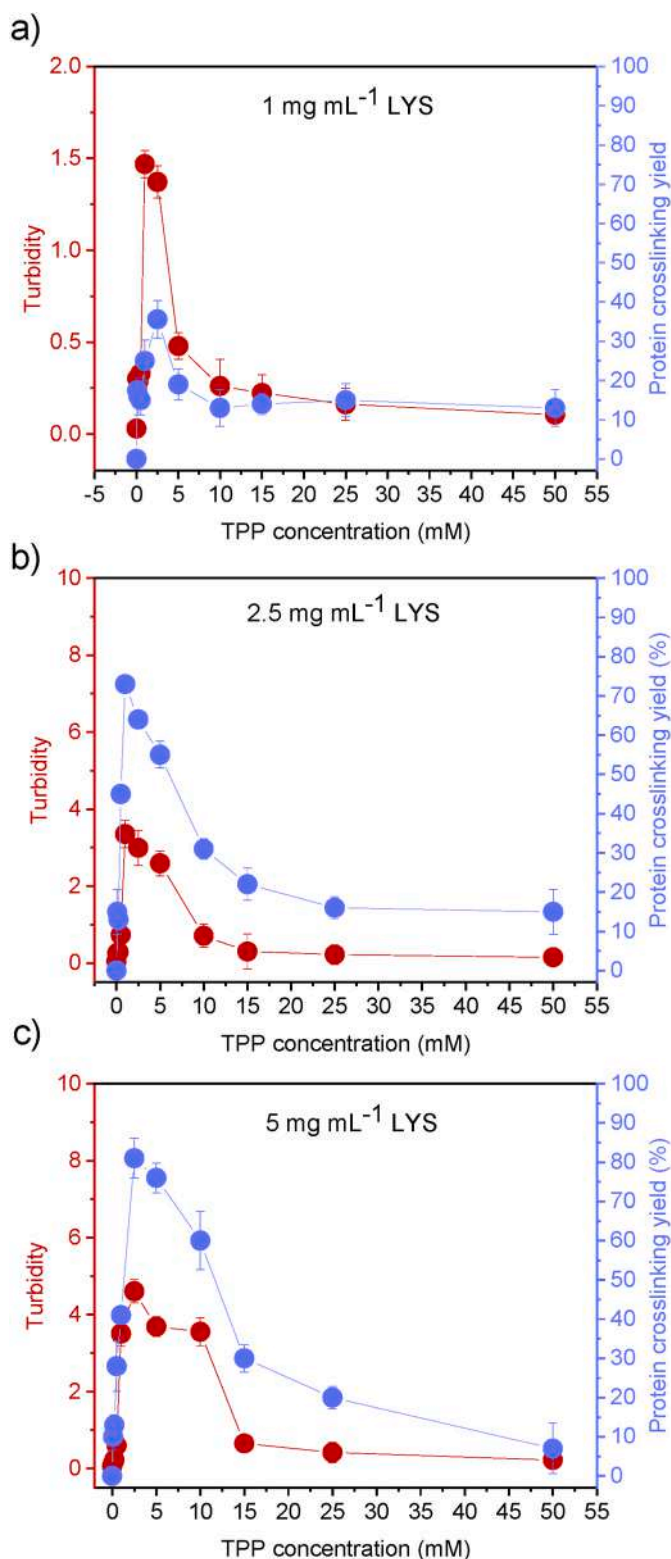


Fig. 3. Evolution of turbidity and protein crosslinking yield as a function of TPP concentration at 1 mg mL⁻¹ (a), 2.5 mg mL⁻¹ (b) and 5 mg mL⁻¹ (c) of LYS.

coacervates are obtained, spherical and micro-sized droplets are observed (Moulik et al., 2022). Instead, precipitates look as irregular and amorphous flocs under the microscope (Archut et al., 2022). Fig. 4 shows images obtained by microscopy for three complexes with LYS/TPP mass ratios of 1.1:1 (1 mg mL⁻¹ LYS, 2.5 mM TPP), 2.7:1 (2.5 mg mL⁻¹ LYS, 2.5 mM TPP), and 5.4:1 (5 mg mL⁻¹ LYS, 2.5 mM TPP). As

can be seen, micron-sized coacervates droplets were observed coexisting with amorphous flocs. Previous studies found a similar coexistence between both configurations for other coacervate systems (Cummings & Obermeyer, 2018; X. Li et al., 2020). For example, Renard and collaborators studied complexes formed by the vegetable protein napin and pectin, observing that coacervate droplets can coexist with amorphous precipitates depending on the mixing ratio (Amine et al., 2019). More recently, Zheng et al. visualized the coexistence of both arrangements for LYS/conglycinin heteroproteins complexes under certain experimental parameters (J. Zheng et al., 2021).

Although some ambiguity can be found in the literature between the terms “coacervates” and “precipitates”, strictly, complex coacervates are those that appear as spherical microdroplets in microscopic observation. Bearing this clarification in mind, and considering that a combination of morphologies was observed microscopically, we cautiously chose to use the term coacervates.

3.2. Effect of pH and salt

The effect of changes in pH and salt was evaluated by turbidity measurements. Fig. 5 summarizes the main results obtained for three complexes with fixed TPP concentration of 2.5 mM and increasing LYS concentration (1, 2.5 and 5 mg mL⁻¹ and LYS:TPP mass ratios of 1.1:1.0, 2.7:1.0 and 5.4:1.0, respectively). As mentioned before, the pH of the solution right after mixing was equal to 9. Turbidity measurements were performed while varying the pH of the solution adding either HCl (from 9 to 4.5) or NaOH (from 9 to 11). The plot in Fig. 5a shows the overlay of all measurements. Starting from pH 9, as pH was forced to decrease, turbidity decreased smoothly up to pH 7 and then abruptly decreased reaching complete disassembly around pH 6.5. As the pH becomes more acidic, the net anionic charge of TPP decreases and the cationic charge of LYS increases. During this process, the loss of charge in TPP molecules by protonation produces the dissociation of complexes and the concomitant decrease in turbidity. However, between pH 9 and 7, the complexes are not totally disassembled thanks to the increase in the cationic character of LYS that favors the stabilization of the complex. At pH > 9, turbidity decreases dramatically until reaching a minimum at pH 10 due to the loss of charge on LYS (amine moieties became deprotonated at alkaline pH). In addition, the effect of pH was also evaluated by maintaining a fixed LYS concentration (2.5 mg mL⁻¹) and varying the concentration of TPP (1, 2.5 and 5 mM of TPP and LYS:TPP mass ratios of 1:0.15, 1:0.37 y 1:0.73, respectively). For all concentrations of TPP under study, a behavior similar to the previous case was observed (Fig. S2a).

Complexes behavior against the addition of salt (NaCl) was evaluated for different concentrations of LYS, keeping the concentration of TPP constant at 2.5 mM (1, 2.5 and 5 mg mL⁻¹ and LYS:TPP mass ratios of 1.1:1, 2.7:1 and 5.4:1, respectively). As shown in Fig. 5b, there is a critical salt concentration where the coacervates are disassembled (turbidity close to 0). The concentration of salt at which the complex is dissolved is known as the salt resistance (L. Li et al., 2018). As can be observed in the plot, the salt resistance increases with the concentration of LYS. More precisely, for 1, 2.5 and 5 mg mL⁻¹ of LYS the salt resistances were 15, 25 and 35 mM, respectively. The dissolution of complexes by addition of monovalent salts is a commonly seen effect that can be explained in terms of counterion replacement (i.e., sodium and chloride anions provoke the disruption of intrinsic ion pairs between amine groups in LYS and TPP anions, destabilizing the complex). Therefore, at higher LYS concentrations, more chloride ions are needed to achieve the disassembly, compared to a lower protein concentration. In addition, ionic strength effect was examined keeping the LYS concentration fixed (2.5 mg mL⁻¹) while varying TPP concentration (1, 2.5 and 5 mM and mass ratio of 1:0.15, 1:0.37 y 1:0.73, respectively). Here, for 1 and 5 mM TPP, complexes are disassembled before in comparison with 2.5 mM TPP (Fig. S2b). For the lower concentration of TPP, the weakening of LYS/TPP interactions in the presence of salt is higher

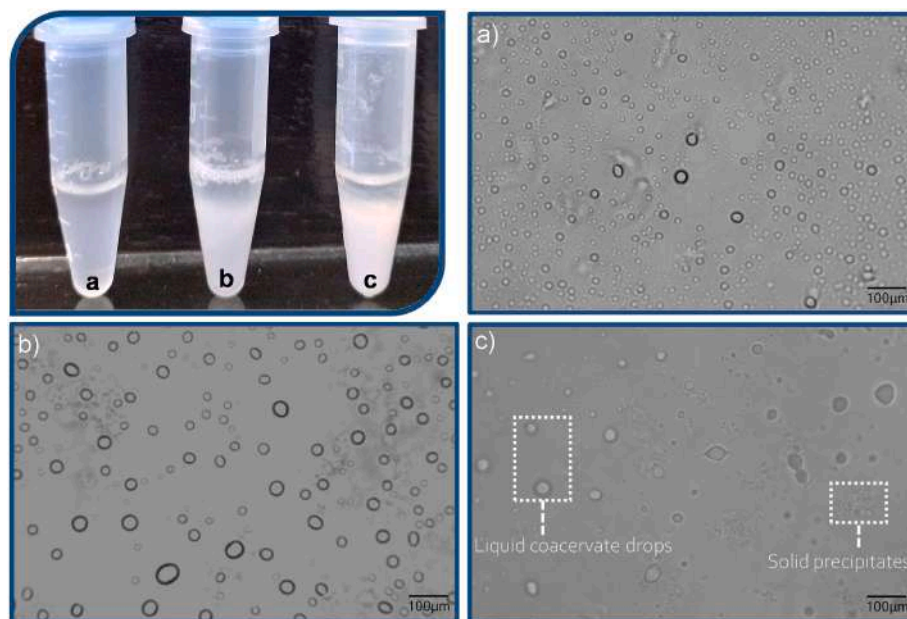


Fig. 4. Images obtained by optical microscopy for different LYS/TPP complexes (pH 9): a) 1 mg mL⁻¹ LYS, 2.5 mM TPP, 1.1:1 LYS/TPP b) 2.5 mg mL⁻¹ LYS, 2.5 mM TPP, 2.7:1 LYS/TPP and c) 5 mg mL⁻¹ LYS, 2.5 mM TPP, 5.4:1 LYS/TPP.

compared to 2.5 mM TPP (less chloride ions are needed to displace TPP anions). For the case of 5 mM TPP, the behavior can be explained considering that, in these conditions, there is less LYS assembled in the complexes in comparison to the complexes obtained with 2.5 mM TPP (see Fig. 3). At 5 mM TPP, the lower content of crosslinked LYS implies that there are less ion pairs to disrupt, therefore, the salt resistance decreases.

The morphology of LYS/TPP complexes at different pH and ionic strength was also explored by optical microscopy (Figs. S3 and S4). A coexistence between the two states of liquid-liquid and solid-liquid separation was observed again, but it was observed that changes in pH and ionic strength could have an impact on the predominance of each conformation. Liquid coacervates seems to be favored at acidic pHs and increasing ionic strengths. Although the mechanism behind the competition between liquid coacervates and solid precipitates is outside the scope of the present work, this result can be explained in terms of the interaction strength between LYS and TPP as: 1) the decrease in pH produces the protonation of phosphate groups in TPP, therefore, weakening the interaction between LYS and TPP, and 2) the disruption of intrinsic ion pairs and formation of extrinsic ion pairs by the presence of NaCl produces the uptake of water molecules from the surroundings, therefore, producing a more hydrated complex (Tirrell, 2018; Y. Zhang et al., 2018). Previously, different authors have observed that the competition between the two conformations of complexes can be modulated by pH changes or salt addition (Amine et al., 2019; Cummings & Obermeyer, 2018; Vieregge et al., 2018). In particular, LYS/ β -lactoglobulin heteroprotein complex have been shown to display a transition from a solid form (at pH 7) to a liquid form (at pH 6.8) due to the reduction of the charge of β -lactoglobulin, leading to a weaker electrostatic interaction (Ainis et al., 2019). A similar behavior was reported for LYS/conglycinin complexes as a solid-liquid transition was observed from pH 8 to pH 6, dominated by a reduction in the number of conglycinin charges (J. Zheng et al., 2021). In addition, LYS/conglycinin complexes exhibit solid-to-liquid phase transition in the presence of NaCl (J. Zheng et al., 2022b; 2022a).

3.3. Encapsulation and protection of curcumin

Complex coacervation is one of the simplest and most sustainable microencapsulation methods because it is based on straightforward

mixing of the components at room temperature and in aqueous solutions. Here, LYS/TPP coacervates are proposed to act with a dual functionality: 1) as encapsulants of CUR to overcome the limitation of poor water solubility, and 2) as protective matrices to improve CUR stability under certain environmental conditions (aqueous long-term storage and light irradiation). Previously, alternative LYS-based complexes were exploited to encapsulate and protect CUR. Li and co-workers efficiently encapsulated CUR in micro-complexes of LYS assembled with polysaccharides such as carboxymethylcellulose and k-carrageenan (Z. Li et al., 2015; Xu et al., 2014). More recently, Gao et al. demonstrated that heteroprotein complex coacervates and precipitates of LYS and β -conglycinin exhibit high CUR loading efficiencies over a broad spectrum of components and cargo molecules concentrations (J. Zheng et al., 2022).

Here, the encapsulation capacity of LYS/TPP coacervates was examined under different experimental conditions. CUR was added to the LYS solution from a stock solution in ethanol before complexation with TPP. It should be mentioned that the presence of CUR and ethanol did not considerably modify the previously discussed properties of the complexes. Fig. 6b shows the phase separation for LYS/TPP complexes (2.5 mg mL⁻¹ LYS, 2.5 mM TPP and LYS:TPP mass ratio of 1:0.37) at different concentrations of CUR. By visually observing the partition of CUR in the two phases, it can be verified that CUR is efficiently encapsulated in the coacervate phase. The efficient loading of CUR in the coacervate droplets was also observed by microscopy (Fig. 6c). In addition, encapsulation can also be visualized in the precipitated complexes. In previous reports, different authors observed that CUR can bind to different proteins (including LYS) through hydrophobic interactions (Somu & Paul, 2021). Moreover, CUR at pH 9 acquires a negative charge due to the deprotonation of one of its hydroxyl groups (Fig. 6a) (Tønnesen & Karlsen, 1985; B. Zheng & McClements, 2020). Therefore, CUR molecules can also enhance their encapsulation by electrostatic interaction with cationic moieties of LYS.

The encapsulation efficiency was further analyzed quantitatively as a function of different variables, i.e., CUR concentration and LYS concentration. Fig. 6d shows the CUR encapsulation efficiency of the LYS/TPP system at different CUR concentrations (ranging from 10 to 500 μ g mL⁻¹) using a constant TPP concentration and three different LYS concentrations (1, 2.5, and 5 mg mL⁻¹). The CUR encapsulation efficiency was found to increase monotonically with CUR concentration,

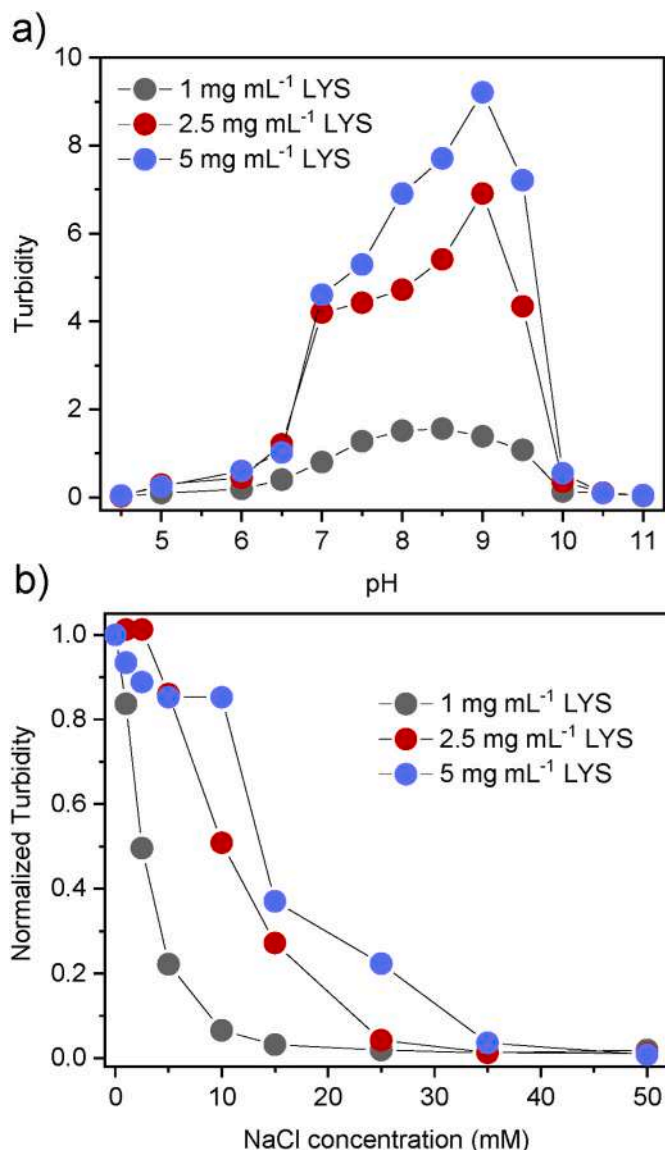


Fig. 5. Evolution of turbidity of LYS/TPP complexes (2.5 mM TPP and LYS/TPP mass ratio of 1.1:1, 2.7:1 and 5.4:1) as a function of (a) pH and (b) NaCl concentration.

reaching a plateau of 80–90% for $[CUR] \sim 250 \mu\text{g mL}^{-1}$ for all LYS concentrations. This result appears to be counterintuitive since one would expect that an increase in CUR concentration will produce a decreasing of the cargo loading by saturation of binding sites. Zheng et al. found a small increase in encapsulation efficiency for the LYS/conglycinin system when the CUR concentration was increased from 130 to 250 mg mL^{-1} at three pH values (6, 7 and 8) (J. Zheng, Gao, Ge, Sun, et al., 2022). In contrast, we observed a substantial increase in the encapsulation rates as the concentration of CUR increased. As encapsulation experiments were carried out at pH 9, CUR can actually function as an anionic crosslinker due its net negative charge ($\text{pKa}_1 = 8.31$, $\text{pKa}_2 = 10.0$, $\text{pKa}_3 = 10.2$) (Leung et al., 2008). Therefore, CUR can be considered as a third component in the formation of the coacervate. In other words, in the presence of CUR, the coacervate phase is composed not only by ion pairs of LYS and TPP but also by ion pairs between LYS and CUR, this last, enhanced by hydrophobic interactions. To evaluate the interaction between CUR and LYS, absorption spectra of CUR (at concentrations of 10, 15, and 25 $\mu\text{g mL}^{-1}$) were recorded at pH 7 (where the net charge of CUR is 0) and pH 9 (where the net charge of CUR is -1). The results are presented in Fig. S5, which shows that at pH 7, the

spectral band position does not exhibit appreciable changes, except for a small hypochromic shift of 2 nm observed for 25 $\mu\text{g mL}^{-1}$ of CUR. However, at alkaline pH, hypochromic shifts of 7 and 12 nm were recorded for 10 and 25 $\mu\text{g mL}^{-1}$ of CUR, respectively. At 15 $\mu\text{g mL}^{-1}$ of CUR, a minor shift of approximately 2 nm was found. Taken together, these results confirm the electrostatic interaction between LYS and CUR and suggest that the formation of LYS/CUR complexes at pH 9 depends on the concentration of CUR. Previously, Lapitsky et al. observed a similar trend in the encapsulation efficiencies of polyallylamine/TPP coacervates with anionic cargo molecules such as the therapeutic ibuprofen and the dye Fast Green FCF. (de Silva et al., 2018; Lawrence et al., 2016). Moreover, Nguyen et al. demonstrated that CUR interacts strongly with polycations in aqueous solutions (M.-H. Nguyen et al., 2016; M. H. Nguyen et al., 2015) On the other hand, it was demonstrated that poorly charged hydrophobic molecules like ciprofloxacin can effectively act as crosslinkers of polycations (Cheow & Hadinoto, 2012; Yu & Hadinoto, 2017). In a similar way that the protein crosslinking yield increased dramatically when raising TPP concentration from 0 to 5 mM (see Fig. 3), the CUR encapsulation efficiency (which in the context of a three-component coacervate can be thought as the CUR crosslinking yield) increase dramatically from 0 to 250 $\mu\text{g mL}^{-1}$ (0.65 mM CUR). According to the typical behavior of multivalent molecule-based complex coacervates (Herrera et al., 2023), all multivalent molecules must overcome a minimum concentration in order to act as ionic crosslinkers of polycations. This could be the main cause for the burst of CUR loading around 250 $\mu\text{g mL}^{-1}$. In addition, there could be competition for the LYS binding site between CUR and TPP, which may also explain the dependence of the encapsulation rates on the concentration of CUR. Specifically, at higher concentrations, the displacement of CUR by TPP may be less significant, leading to increased encapsulation.

The effect of TPP concentration on CUR encapsulation for the three LYS concentrations (1, 2.5, and 5 mg mL^{-1}) is depicted in Fig. 6e. For all three cases, a decrease in encapsulation was observed with an increase in TPP concentration. This behavior may be due to the decrease in the protein crosslinking yield with increasing TPP concentration (Fig. 3). In parallel, TPP can compete with CUR for binding sites on the protein, decreasing the payload encapsulation.

Other LYS-based coacervate complexes have reported maximum encapsulation efficiencies of about 90%. For example, Zheng et al. reported encapsulation efficiencies of close to 95% for LYS/conglycinin complexes (J. Zheng et al., 2022). Li et al. found that LYS/CMC coacervates can load CUR with efficiencies of around 99% (Z. Li et al., 2015). In addition, complexes formed by other macromolecules have exhibited efficiencies greater than 90%, such as gum arabic/bovine serum albumin complexes (92%) (Shahgholian & Rajabzadeh, 2016), gum Arabic/whey protein complexes (98.88%) (Mohammadian et al., 2019), pea protein isolate/high methoxyl pectin complexes (97.33%) (Guo et al., 2020), and mung bean protein and succinylated chitosan complexes (89%) (Mirmohammad Meiguni et al., 2022). On the other hand, the level of encapsulation efficiency obtained in the present study was significantly higher than that of many other types of carriers. For example, complex coacervates of LYS and κ -carrageenan exhibited an encapsulation efficiency of about 71% (Xu et al., 2014), while gliadin and sodium alginate complexes showed an efficiency of 81% (Su et al., 2021). Additionally, nanocomplexes of bovine serum albumin and poly-D-lysine presented an encapsulation efficiency of 60% (Maldonado et al., 2017). Recently, we report an encapsulation efficiency of 60% for poly-L-lysine dendrigraft/TPP nanocomplexes (Agazzi et al., 2020).

To evaluate the protective performance of the complexes, the stability of CUR was monitored under long-term storage conditions in aqueous solutions and under irradiation with visible light. For these studies, LYS/TPP complex with a mass ratio of 1:0.37 (2.5 mg mL^{-1} LYS and 2.5 mM TPP) and a CUR concentration of 250 $\mu\text{g mL}^{-1}$ were selected. Firstly, complexes with CUR and corresponding controls (aqueous solutions at pH 9 of CUR free, CUR/LYS and CUR/TPP) were

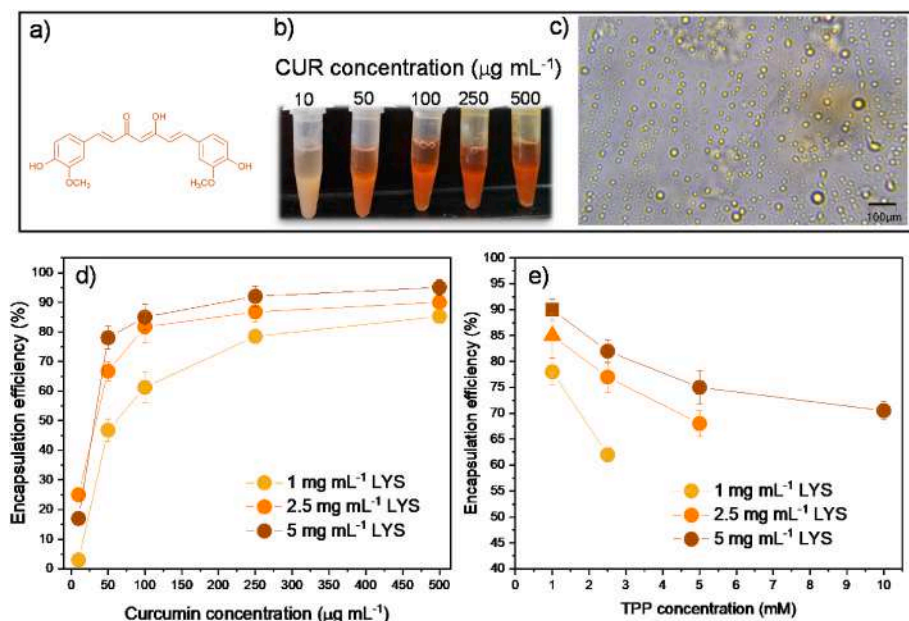


Fig. 6. (a) Chemical structure of CUR, (b) Real image of phase separation for LYS/CUR/TPP (2.5 mg mL⁻¹ LYS, 2.5 mM TPP and LYS:TPP mass ratio of 1:0.37) complexes at different CUR concentrations, (c) Image obtained by optical microscopy of LYS/CUR/TPP (2.5 mg mL⁻¹ LYS, 2.5 mM TPP and 100 µg mL⁻¹ CUR) complexes; (d) Encapsulation efficiency as a function of CUR and LYS concentrations for different complexes (2.5 mM TPP) and (e) Encapsulation efficiency of CUR (100 µg mL⁻¹) as a function of TPP concentration for different complexes at three LYS concentrations (1, 2.5 and 5 mg mL⁻¹).

stored at 4 °C in the dark for 1, 5, 10, 15 and 20 days. Fig. 7a shows the percentage of CUR preservation as a function of time for each sample. The LYS/TPP coacervates presented an enhanced protective capacity, showing a preservation percentage close to 90% after 20 days of storage. The LYS/CUR control assay also showed little degradation (82% of preservation at 20 days), possibly due to hydrophobic and electrostatic interactions between CUR and LYS that could improve the molecules stability. Other studies have reported the ability of coacervates to stabilize CUR during long-term storage. For instance, CUR encapsulated in LYS/conglycinin coacervates at alkaline pH was preserved at 67% after 14 days of storage at 4 °C (J. Zheng et al., 2022). In addition, Mohammadian et al. observed visually that the appearance of CUR loaded in complex coacervates made of gum arabic and whey protein nanofibrils remained unchanged after 15 days (Mohammadian et al., 2019).

Finally, the effect of light on the encapsulated CUR was explored using a visible light irradiation lamp at two intervals of irradiation (2.5 h y 5 h). It is known that CUR is easily degradable by light, causing it to lose its functional properties (Priyadarsini, 2009; B. Zheng & McClements, 2020). Previously, LYS/conglycinin and LYS/κ-carrageenan complexes showed the ability to act as light screens and improved the chemical stability of CUR (Xu et al., 2014; J. Zheng et al., 2022). As can be seen in Fig. 7b, the lowest photo-degradation rate was observed for the CUR encapsulated in coacervates. After 5 h of irradiation, CUR preservation percentages for CUR free, CUR/TPP, and CUR/LYS were 26%, 28%, and 31%, respectively. Instead, CUR trapped in the complexes showed a preservation of 55%, indicating that LYS/TPP coacervates can prolong the lifetime of the bioactive agent in aqueous conditions under visible light irradiation. The protection mechanism is possibly due to the fact that coacervates act as a thick barrier that decreases the penetration and impact of light on CUR molecules (Guo et al., 2020).

Although comparing different systems is challenging due to variations in irradiation conditions such as sources, intensity, and distance between lamp and sample, the light shielding capacity provided by our system is comparable to that observed for other complexes. For instance, light-protective ability of LYS/conglycinin complexes was evaluated at pH 8 for CUR. They observed that after 5 h of simulated light irradiation, the preservation rate of CUR was 78%. However, after 3 h of sunlight exposure, the preservation rate dropped to 30% (J. Zheng et al., 2022). Salami and co-workers found that CUR encapsulated in gum Arabic/whey protein complexes remained 80% intact after 15 days of visible

light irradiation (Mohammadian et al., 2019). The same authors observed about 60% preservation of CUR in complexes of mung bean protein and succinylated chitosan (Mirmohammad Meiguni et al., 2022).

3.4. Lysozyme enzyme activity

First, the effect of TPP complexation on the antibacterial activity of LYS was analyzed. For this, the growth inhibition of *M. luteus* was monitored by measuring the decrease in the OD600nm of cell cultures by adding TPP (2.5 mM), LYS (5 mg mL⁻¹), LYS/TPP complexes (5 mg mL⁻¹ LYS, 2.5 mM TPP) and LYS/TPP disassembled (see section 2.9). Fig. 8 summarizes the results obtained. As can be seen, both LYS/TPP complexes and disassembled LYS/TPP complexes showed a decrease in OD600nm similar to that observed for LYS free. Furthermore, no inhibitory activity was detected for TPP alone. This result indicates the enzymatic activity of LYS is not significantly affected by the presence of TPP.

As a supplementary analysis, the possible presence of biofilms on the walls of the previously prepared treatment tubes was qualitatively assessed after 16 h. Formation of biofilms with intense yellow color was observed on the control tube and the TPP tube (Fig. S6). However, for the treatments that included LYS (LYS, LYS/TPP complexes, and disassembled LYS/TPP), a lower formation was visualized. In addition, a bleaching of the strains was noted in the presence of the enzyme samples, resulting in a whitish color instead of the characteristic yellow pigment. Notably, the samples with LYS/TPP and disassembled LYS/TPP complexes showed a similar reduction in biofilm formation as observed with LYS alone. This observation reinforces what was previously discussed regarding the negligible effect of ionic complexation on the enzymatic activity of LYS. It has been determined that antimicrobial compounds could act as signaling molecules with an effect on the modulation of some functions such as biofilm formation, pigmentation, metabolite production, motility, among others (Das & Mehta, 2018; Latimer et al., 2012; Romero et al., 2011).

Previous studies showed different behaviors regarding the persistence of LYS enzymatic activity after coacervation. Several reports indicated that the antibacterial activity was reduced after coacervation with low methoxyl pectin, sodium alginate, carboxymethyl cellulose and *Arthrospira platensis* protein (Amara et al., 2016; Bayarri et al., 2014; Benelhadj et al., 2016; Wang et al., 2021). This activity decline may be

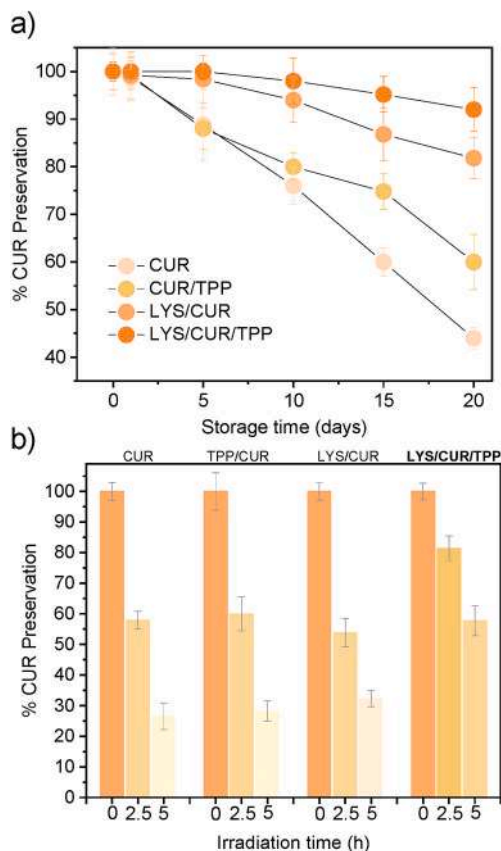


Fig. 7. Percentage of preservation of CUR as a function of storage time (5 °C in the dark) (a) and irradiation time with visible light (b) in samples of CUR (250 $\mu\text{g mL}^{-1}$), TPP/CUR (2.5 mM TPP, 250 $\mu\text{g mL}^{-1}$ CUR), LYS/CUR (2.5 mg mL^{-1} LYS, 250 $\mu\text{g mL}^{-1}$ CUR) and LYS/CUR/TPP complexes (2.5 mg mL^{-1} LYS, 250 $\mu\text{g mL}^{-1}$ CUR and 2.5 mM TPP).

caused by a steric hindrance between LYS active sites and its substrate (bacteria cell wall) generated by LYS aggregation. However, other studies showed that the antibacterial activity of LYS is little affected by complexation. Recently, it was reported that, under certain experimental conditions, LYS complexed with conglycinin and carboxymethyl konjac glucomannan retain the lytic activity (J. Zheng et al., 2021).

3.5. Curcumin antibacterial activity

The antibacterial capacity of the encapsulated CUR at three concentrations (50, 250 and 500 $\mu\text{g mL}^{-1}$) was evaluated against different strains of *S. aureus* (ATCC 25923, DM1 and DM2). *S. aureus* is a Gram-positive bacterium frequently causing foodborne disease (Kadariya et al., 2014). LYS (2.5 mg mL^{-1}), TPP (2.5 mM), LYS/TPP complexes (2.5 mg mL^{-1} LYS, 2.5 mM TPP) and CUR (50, 250 and 500 $\mu\text{g mL}^{-1}$) were applied as controls. For the three strains, only the regions where the complexes/CUR were deposited showed bacterial growth inhibition (Fig. 9). In all cases, a growth inhibition halo of approximately 1 cm in diameter was observed. Surprisingly, under these experimental conditions the samples with LYS did not show an appreciable antibacterial effect. Possibly, the enzyme presents little diffusion in the agarized medium, limiting its antibacterial activity. The size of the growth inhibition halo is influenced by different factors, including the diffusion capacity of the compound (Balouiri et al., 2016).

The antibacterial activity of CUR free (250 $\mu\text{g mL}^{-1}$ CUR) in water and trapped in coacervates (2.5 mg mL^{-1} LYS, 250 $\mu\text{g mL}^{-1}$ CUR, 2.5 mM TPP) was tested against *S. aureus* ATCC 25923. CUR showed very little antibacterial effect at all three concentrations (Fig. 9d, circles 1, 2 and 3). This may be due to the poor dispersibility in an aqueous medium

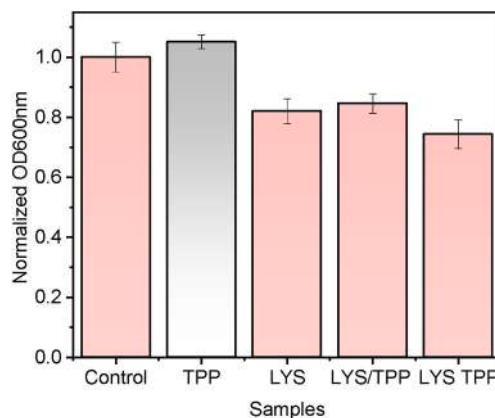


Fig. 8. OD600nm of *M. luteus* cultures after 90 min incubation with different samples: Control (*M. luteus* 10⁶ CFU mL^{-1}), TPP (2.5 mM), LYS (5 mg mL^{-1}), LYS/TPP (5 mg mL^{-1} LYS, 2.5 mM TPP) and disassembled LYS/TPP.

that affects its diffusion in an agarized medium (Anand et al., 2007; Somu & Paul, 2021). Interestingly, LYS/CUR/TPP complexes after 20 days of storage continued to show inhibition to bacteria growth (Fig. 9d, circle 5). Instead, CUR alone under the same storage time and conditions showed no activity (Fig. 9d, circle 4). These results are consistent with those previously presented (Fig. 7a) where it was observed that the complexes enhance the long-term stability of the CUR in aqueous medium. Taken all together, these results indicate that the complexes

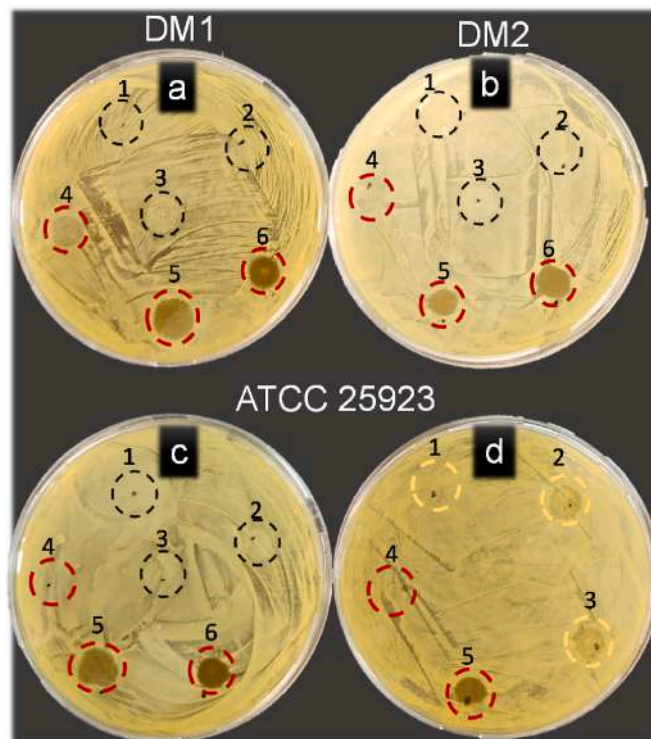


Fig. 9. Antibacterial activity of the complexes LYS/CUR/TPP against *S. aureus* DM1 (a), DM2 (b) and ATCC 25923 (c and d). For (a), (b) and (c): 1) LYS; 2) TPP; 3) LYS/TPP; 4) LYS/CUR/TPP (50 $\mu\text{g mL}^{-1}$ CUR); 5) LYS/CUR/TPP (250 $\mu\text{g mL}^{-1}$ CUR); 6) LYS/CUR/TPP (500 $\mu\text{g mL}^{-1}$ CUR). For (d) 1) CUR (50 $\mu\text{g mL}^{-1}$); 2) CUR (250 $\mu\text{g mL}^{-1}$); 3) CUR (500 $\mu\text{g mL}^{-1}$); 4) CUR (50 $\mu\text{g mL}^{-1}$ CUR in water/5% ethanol) after 20 days of storage and 5) LYS/CUR/TPP (250 $\mu\text{g mL}^{-1}$ CUR) after 20 days of storage. In all cases the concentrations of LYS and TPP were 2.5 mg mL^{-1} and 2.5 mM, respectively. All samples were prepared in water/5% ethanol.

significantly improve and preserve the antibacterial activity of CUR in aqueous media.

The antibacterial effect of CUR in the complexes was also analyzed using the growth delay curve assay. The growth curves of *S. aureus* exposed to different treatments are depicted in Fig. S7. The growth curve (GC) plots showed the normal growth pattern of the microorganism under the experimental conditions. When culture was exposed to free LYS and LYS/TPP complexes, the growth pattern was similar to (GC), confirming previous findings from microbiological studies conducted on solid medium (Fig. 9). In contrast, when cultures were exposed to free CUR and CUR encapsulated in the complexes, they did not reach the exponential phase even after 12 h. This result indicates that the complexes do not affect the antibacterial activity of CUR in the free liquid culture medium. Intriguingly, after 24 h of incubation, only the encapsulated CUR continued to inhibit growth (Fig. S7B). In contrast, in the presence of free CUR, the bacteria exhibited growth after this prolonged incubation period. This discrepancy suggests that the treatment with LYS/CUR/TPP complexes exerts a bactericidal effect on *S. aureus*, whereas free CUR displays a bacteriostatic action. This difference may be attributed to the aggregation of CUR, which exhibits slight solubility in an aqueous medium over extended time periods.

4. Conclusion

In this work, we evaluated for the first time the carrier properties of single-macromolecule complex coacervates based on the direct mixing of two food additives: protein LYS and multivalent anion TPP. Physicochemical studies indicated that the occurrence and performance of the two-phase separation is strongly dependent on the concentrations of components, ionic strength and pH. Furthermore, it was observed that in the concentrated phase, the complexes exhibit a combination of two physical configurations: liquid complex coacervates and amorphous solid precipitates. Preliminary studies indicated that the dominance of each of these morphologies could be modulated by changes in pH and ionic strength. On the other hand, it was confirmed that enzymatic activity of LYS is not affected by complexation with TPP.

The encapsulation capacities of the complexes were evaluated using CUR. The results showed that LYS/TPP coacervates are highly efficient to encapsulate and stabilize the bioactive agent under long storage conditions and irradiation of visible light. In addition, it was observed that the encapsulation of CUR optimizes its antibacterial performance. In summary, we believe that bioactive LYS/TPP complexes present attractive properties to act as encapsulants and protectors of functional agents (particularly CUR) for foodtech applications. This first report on LYS/TPP complexes as a platform for microencapsulation opens the way for future studies that focus on different aspects of these materials such as: comprehensive evaluation of the properties and formation yield of coacervates by modulating the components mass ratios and the initial pH, film-forming properties and complexes behavior in food matrices, encapsulation and co-encapsulation of other food additives, powder formulation by applying processing techniques such as freeze or spray drying, among others.

Credit author statement

Maximiliano L. Agazzi: Conceptualization, Methodology, Investigation, Data Curation, Writing - Review & Editing. M. Fernanda Paletti Rovey: Methodology, Investigation, Data Curation, Writing - Review & Editing. Eugenia Apuzzo: Methodology, Investigation. Santiago E. Herrera: Conceptualization, Methodology, Writing - Review & Editing; Visualization. Mariana B. Spesia: Methodology, Investigation, Writing - Review & Editing, Resources. M. de las Mercedes Oliva: Writing - Review & Editing, Supervision, Resources. Omar Azzaroni: Conceptualization, Writing - Review & Editing, Supervision, Resources, Funding acquisition.

Declaration of competing interest

None

Data availability

No data was used for the research described in the article.

Acknowledgments

E.A. and M.F.P. acknowledges a scholarship from CONICET. OA acknowledges financial support from Universidad Nacional de La Plata (PPID-X867), CONICET (PIP 0370), and ANPCyT (PICT2018-00780). M. M.O. acknowledge the financial support from Universidad Nacional de Río Cuarto (PPI 2020–2022. Res. 083/20). M.B.S. acknowledge the financial support from ANPCYT (PICT N° 1482/19) S.E.H, M.L.A, M.B.S., M.M.O. and O.A. are CONICET fellows.

Appendix A. Supplementary data

Supplementary data to this article can be found online at <https://doi.org/10.1016/j.foodhyd.2023.109134>.

References

- Agazzi, M. L., Herrera, S. E., Cortez, M. L., Marmisollé, W. A., & Azzaroni, O. (2020). Self-assembled peptide dendrigraft supraparticles with potential application in pH/enzyme-triggered multistage drug release. *Colloids and Surfaces B: Biointerfaces*, 190, Article 110895. <https://doi.org/10.1016/j.colsurfb.2020.110895>
- Agazzi, M. L., Herrera, S. E., Cortez, M. L., Marmisollé, W. A., Tagliazucchi, M., & Azzaroni, O. (2020). Insulin delivery from glucose-responsive, self-assembled, polyamine nanoparticles: Smart "sense-and-treat" nanocarriers made easy. *Chemistry - A European Journal*, 26(11), 2456–2463. <https://doi.org/10.1002/chem.201905075>
- Agazzi, M. L., Herrera, S. E., Cortez, M. L., Marmisollé, W. A., von Bilderling, C., Pietrasanta, L. I., & Azzaroni, O. (2019). Continuous assembly of supramolecular polyamine-phosphate networks on surfaces: Preparation and permeability properties of nanofilms. *Soft Matter*, 15(7), 1640–1650. <https://doi.org/10.1039/C8SM02387E>
- Ainis, W. N., Boire, A., Solé-Jamault, V., Nicolas, A., Bouhallab, S., & Ipsen, R. (2019). Contrasting assemblies of oppositely charged proteins. *Langmuir*, 35(30), 9923–9933. <https://doi.org/10.1021/acs.langmuir.9b01046>
- Alam, S. S., Mather, C. B., Seo, Y., & Lapitsky, Y. (2021). Poly(allylamine)/tripolyphosphate coacervates for encapsulation and long-term release of cetylpyridinium chloride. *Colloids and Surfaces A: Physicochemical and Engineering Aspects*, 629, Article 127490. <https://doi.org/10.1016/j.colsurfa.2021.127490>
- Alam, S. S., Seo, Y., & Lapitsky, Y. (2020). Highly sustained release of bactericides from complex coacervates. *ACS Applied Bio Materials*, 3(12), 8427–8437. <https://doi.org/10.1021/acsbm.0c00763>
- Amara, C. B., Degraeve, P., Oulahal, N., & Gharsallaoui, A. (2017). pH-dependent complexation of lysozyme with low methoxyl (LM) pectin. *Food Chemistry*, 236, 127–133. <https://doi.org/10.1016/j.foodchem.2017.03.124>
- Amara, C. B., Eghbal, N., Oulahal, N., Degraeve, P., & Gharsallaoui, A. (2016). Properties of lysozyme/sodium alginate complexes for the development of antimicrobial films. *Food Research International*, 89, 272–280. <https://doi.org/10.1016/j.foodres.2016.08.015>
- Amine, C., Boire, A., Kermaerrec, A., & Renard, D. (2019). Associative properties of rapeseed napin and pectin: Competition between liquid-liquid and liquid-solid phase separation. *Food Hydrocolloids*, 92, 94–103. <https://doi.org/10.1016/j.foodhyd.2019.01.026>
- Anand, P., Kunnumakkara, A. B., Newman, R. A., & Aggarwal, B. B. (2007). Bioavailability of curcumin: Problems and promises. *Molecular Pharmacology*, 4(6), 807–818. <https://doi.org/10.1021/mp700113r>
- Anema, S. G., de Kruijff, C. G., & Kees, (2013). Coacervates of lysozyme and β -casein. *Journal of Colloid and Interface Science*, 398, 255–261. <https://doi.org/10.1016/j.jcis.2013.02.013>
- Antonov, Y. A., & Zhuravleva, I. L. (2020). Gum Arabic/Lysozyme coacervate phase similar in structure to multilamellar liposomes. *Food Hydrocolloids*, 105, Article 105749. <https://doi.org/10.1016/j.foodhyd.2020.105749>
- Antonov, Y. A., Zhuravleva, I., Volodine, A., Moldenaers, P., & Cardinaels, R. (2017). Effect of the helix-coil transition in bovine skin gelatin on its associative phase separation with lysozyme. *Langmuir*, 33(47), 13530–13542. <https://doi.org/10.1021/acs.langmuir.7b01477>
- Archut, A., Drusch, S., & Kastner, H. (2022). Complex coacervation of pea protein and pectin: Effect of degree and pattern of free carboxyl groups on biopolymer interaction. *Food Hydrocolloids*, 133, Article 107884. <https://doi.org/10.1016/j.foodhyd.2022.107884>

- Balouiri, M., Sadiki, M., & Ibensouda, S. K. (2016). Methods for in vitro evaluating antimicrobial activity: A review. *Journal of Pharmaceutical Analysis*, 6(2), 71–79. <https://doi.org/10.1016/j.jpba.2015.11.005>
- Bayarri, M., Oulahal, N., Degraeve, P., & Gharsallaoui, A. (2014). Properties of lysozyme/low methoxyl (LM) pectin complexes for antimicrobial edible food packaging. *Journal of Food Engineering*, 131, 18–25. <https://doi.org/10.1016/j.jfoodeng.2014.01.013>
- Benelhadj, S., Fejji, N., Degraeve, P., Attia, H., Ghorbel, D., & Gharsallaoui, A. (2016). Properties of lysozyme/*Arthrospira platensis* (Spirulina) protein complexes for antimicrobial edible food packaging. *Algal Research*, 15, 43–49. <https://doi.org/10.1016/j.algal.2016.02.003>
- Blocher, W. C., & Perry, S. L. (2017). Complex coacervate-based materials for biomedicine. *WIREs Nanomedicine and Nanobiotechnology*, 9(4). <https://doi.org/10.1002/wnan.1442>
- Bye, J. W., Cowieson, N. P., Cowieson, A. J., Selle, P. H., & Falconer, R. J. (2013). Dual effects of sodium phytate on the structural stability and solubility of proteins. *Journal of Agricultural and Food Chemistry*, 61(2), 290–295. <https://doi.org/10.1021/jf303926v>
- Bye, J. W., & Curtis, R. A. (2019). Controlling phase separation of lysozyme with polyvalent anions. *The Journal of Physical Chemistry B*, 123(3), 593–605. <https://doi.org/10.1021/acs.jpbc.8b10868>
- Chen, K., Zhang, M., Mujumdar, A. S., & Wang, H. (2021). Quinoa protein-gum Arabic complex coacervates as a novel carrier for eugenol: Preparation, characterization and application for minced pork preservation. *Food Hydrocolloids*, 120, Article 106915. <https://doi.org/10.1016/j.foodhyd.2021.106915>
- Cheow, W. S., & Hadinoto, K. (2012). Green amorphous nanoplex as a new supersaturating drug delivery system. *Langmuir*, 28(15), 6265–6275. <https://doi.org/10.1021/la204782x>
- Clinical and Laboratory Standards Institute. (2012). *Performance standards for antimicrobial disk susceptibility tests: Approved standard - eleventh edition* (Vol. 32). Issue 1.
- Comert, F., & Dubin, P. L. (2017). Liquid-liquid and liquid-solid phase separation in protein-polyelectrolyte systems. *Advances in Colloid and Interface Science*, 239, 213–217. <https://doi.org/10.1016/j.cis.2016.08.005>
- Comert, F., Malanowski, A. J., Azarika, F., & Dubin, P. L. (2016). Coacervation and precipitation in polysaccharide-protein systems. *Soft Matter*, 12(18), 4154–4161. <https://doi.org/10.1039/C6SM00044D>
- Cortés-Morales, E. A., Mendez-Montealvo, G., & Velazquez, G. (2021). Interactions of the molecular assembly of polysaccharide-protein systems as encapsulation materials. A review. *Advances in Colloid and Interface Science*, 295, Article 102398. <https://doi.org/10.1016/j.cis.2021.102398>
- Croguennec, T., Tavares, G. M., & Bouhallab, S. (2017). Heteroprotein complex coacervation: A generic process. *Advances in Colloid and Interface Science*, 239, 115–126. <https://doi.org/10.1016/j.cis.2016.06.009>
- Cummings, C. S., & Obermeyer, A. C. (2018). Phase separation behavior of supercharged proteins and polyelectrolytes. *Biochemistry*, 57(3), 314–323. <https://doi.org/10.1021/acs.biochem.7b00990>
- Das, R., & Mehta, D. K. (2018). Microbial biofilm and quorum sensing inhibition: Endowment of medicinal plants to combat multidrug-resistant bacteria. *Current Drug Targets*, 19(16), 1916–1932. <https://doi.org/10.2174/1389450119666180406111143>
- Devi, N., Sarmah, M., Khatun, B., & Maji, T. K. (2017). Encapsulation of active ingredients in polysaccharide-protein complex coacervates. *Advances in Colloid and Interface Science*, 239, 136–145. <https://doi.org/10.1016/j.cis.2016.05.009>
- Eghbal, N., & Choudhary, R. (2018). Complex coacervation: Encapsulation and controlled release of active agents in food systems. *Lebensmittel-Wissenschaft & Technologie*, 90, 254–264. <https://doi.org/10.1016/j.lwt.2017.12.036>
- Friedowitz, S., Lou, J., Barker, K. P., Will, K., Xia, Y., & Qin, J. (2021). Looping-in complexation and ion partitioning in nonstoichiometric polyelectrolyte mixtures. *Science Advances*, 7(31). <https://doi.org/10.1126/sciadv.abg8654>
- Gómez-Estaca, J., Balaguer, M. P., López-Carballo, G., Gavara, R., & Hernández-Muñoz, P. (2017). Improving antioxidant and antimicrobial properties of curcumin by means of encapsulation in gelatin through electrohydrodynamic atomization. *Food Hydrocolloids*, 70, 313–320. <https://doi.org/10.1016/j.foodhyd.2017.04.019>
- Guo, Q., Su, J., Xie, W., Tu, X., Yuan, F., Mao, L., & Gao, Y. (2020). Curcumin-loaded pea protein isolate-high methoxyl pectin complexes induced by calcium ions: Characterization, stability and in vitro digestibility. *Food Hydrocolloids*, 98, Article 105284. <https://doi.org/10.1016/j.foodhyd.2019.105284>
- Herrera, S. E., Agazzi, M. L., Apuzzo, E., Cortez, M. L., Marmisollé, W. A., Tagliacuzzi, M., & Azzaroni, O. (2023). Polyelectrolyte-multivalent molecule complexes: Physicochemical properties and applications. *Soft Matter*, 19(11), 2013–2041. <https://doi.org/10.1039/D2SM01507B>
- Herrera, S. E., Agazzi, M. L., Cortez, M. L., Marmisollé, W. A., Tagliacuzzi, M., & Azzaroni, O. (2019). Polyamine colloids cross-linked with phosphate ions: Towards understanding the solution phase behavior. *ChemPhysChem*, 20(8), 1044–1053. <https://doi.org/10.1002/cphc.201900046>
- Herrera, S. E., Agazzi, M. L., Cortez, M. L., Marmisollé, W. A., Tagliacuzzi, M., & Azzaroni, O. (2020). Redox-active polyamine-salt aggregates as multimistimuli-responsive soft nanoparticles. *Physical Chemistry Chemical Physics*, 22(14), 7440–7450. <https://doi.org/10.1039/D0CP00077A>
- Kadariya, J., Smith, T. C., & Thapaliya, D. (2014). *Staphylococcus aureus* and staphylococcal food-borne disease: An ongoing challenge in public health. *BioMed Research International*, 1–9. <https://doi.org/10.1155/2014/827965>, 2014.
- Khorshidian, N., Khaniri, E., Koushki, M. R., Sohrabvandi, S., & Yousefi, M. (2022). An overview of antimicrobial activity of lysozyme and its functionality in cheese. *Frontiers in Nutrition*, 9. <https://doi.org/10.3389/fnut.2022.833618>
- Kuehner, D. E., Engmann, J., Fergg, F., Wernick, M., Blanch, H. W., & Prausnitz, J. M. (1999). Lysozyme net charge and ion binding in concentrated aqueous electrolyte solutions. *The Journal of Physical Chemistry B*, 103(8), 1368–1374. <https://doi.org/10.1021/jp983852i>
- Kumari, A., Kumari, K., & Gupta, S. (2019). Protease responsive essential amino-acid based nanocarriers for near-infrared imaging. *Scientific Reports*, 9(1), Article 20334. <https://doi.org/10.1038/s41598-019-56871-4>
- Kurtz, I. S., Sui, S., Hao, X., Huang, M., Perry, S. L., & Schiffman, J. D. (2019). Bacteria-resistant, transparent, free-standing films prepared from complex coacervates. *ACS Applied Bio Materials*, 2(9), 3926–3933. <https://doi.org/10.1021/acsabm.9b00502>
- Lampila, L. E. (2013). Applications and functions of food-grade phosphates. *Annals of the New York Academy of Sciences*, 1301(1), 37–44. <https://doi.org/10.1111/nyas.12230>
- Latimer, J., Forbes, S., & McBain, A. J. (2012). Attenuated virulence and biofilm formation in *Staphylococcus aureus* following sublethal exposure to triclosan. *Antimicrobial Agents and Chemotherapy*, 56(6), 3092–3100. <https://doi.org/10.1128/AAC.05904-11>
- Lawrence, P. G., & Lapitsky, Y. (2015). Ionically cross-linked poly(allylamine) as a stimulus-responsive underwater adhesive: Ionic strength and pH effects. *Langmuir*, 31(4), 1564–1574. <https://doi.org/10.1021/la504611x>
- Lawrence, P. G., Patil, P. S., Leipzig, N. D., & Lapitsky, Y. (2016). Ionically cross-linked polymer networks for the multiple-month release of small molecules. *ACS Applied Materials & Interfaces*, 8(7), 4323–4335. <https://doi.org/10.1021/acsami.5b10070>
- Leung, M. H. M., Colangelo, H., & Kee, T. W. (2008). Encapsulation of curcumin in cationic micelles suppresses alkaline hydrolysis. *Langmuir*, 24(11), 5672–5675. <https://doi.org/10.1021/la800780w>
- Li, X., Erni, P., van der Gucht, J., & de Vries, R. (2020). Encapsulation using plant proteins: Thermodynamics and kinetics of wetting for simple zein coacervates. *ACS Applied Materials & Interfaces*, 12(13), 15802–15809. <https://doi.org/10.1021/acsami.9b20746>
- Li, L., Srivastava, S., Andreev, M., Marciel, A. B., de Pablo, J. J., & Tirrell, M. V. (2018). Phase behavior and salt partitioning in polyelectrolyte complex coacervates. *Macromolecules*, 51(8), 2988–2995. <https://doi.org/10.1021/acs.macromol.8b00238>
- Li, Z., Wang, Y., Pei, Y., Xiong, W., Zhang, C., Xu, W., Liu, S., & Li, B. (2015). Curcumin encapsulated in the complex of lysozyme/carboxymethylcellulose and implications for the antioxidant activity of curcumin. *Food Research International*, 75, 98–105. <https://doi.org/10.1016/j.foodres.2015.05.058>
- Maldonado, L., Sadeghi, R., & Kokini, J. (2017). Nanoparticulation of bovine serum albumin and poly-D-lysine through complex coacervation and encapsulation of curcumin. *Colloids and Surfaces B: Biointerfaces*, 159, 759–769. <https://doi.org/10.1016/j.colsurfb.2017.08.047>
- Marciel, A. B., Chung, E. J., Brettmann, B. K., & Leon, L. (2017). Bulk and nanoscale polypeptide based polyelectrolyte complexes. *Advances in Colloid and Interface Science*, 239, 187–198. <https://doi.org/10.1016/j.cis.2016.06.012>
- Meng, S., Ting, J. M., Wu, H., & Tirrell, M. V. (2020). Solid-to-Liquid phase transition in polyelectrolyte complexes. *Macromolecules*, 53(18), 7944–7953. <https://doi.org/10.1021/acs.macromol.0c00930>
- Mirmohammad Meiguni, M. S., Salami, M., Rezaei, K., Ghaffari, S., Aliyari, M. A., Emam-Djomeh, Z., Barazandegan, Y., & Gruen, I. (2022). Curcumin-loaded complex coacervate made of mung bean protein isolate and succinylated chitosan as a novel medium for curcumin encapsulation. *Journal of Food Science*, 87(11), 4930–4944. <https://doi.org/10.1111/1750-3841.16341>
- Mohammadian, M., Salami, M., Alavi, F., Momen, S., Emam-Djomeh, Z., & Moosavi-Movahedi, A. A. (2019). Fabrication and characterization of curcumin-loaded complex coacervates made of gum Arabic and whey protein nanofibrils. *Food Biophysics*, 14(4), 425–436. <https://doi.org/10.1007/s11483-019-09591-1>
- Monteiro, A. A., Monteiro, M. R., Pereira, R. N., Diniz, R., Costa, A. R., Malcata, F. X., Teixeira, J. A., Teixeira, Á. V., Oliveira, E. B., Coimbra, J. S., Vicente, A. A., & Ramos, Ó. L. (2016). Design of bio-based supramolecular structures through self-assembly of α -lactalbumin and lysozyme. *Food Hydrocolloids*, 58, 60–74. <https://doi.org/10.1016/j.foodhyd.2016.02.009>
- Moschakis, T., & Biliaderis, C. G. (2017). Biopolymer-based coacervates: Structures, functionality and applications in food products. *Current Opinion in Colloid & Interface Science*, 28, 96–109. <https://doi.org/10.1016/j.cocis.2017.03.006>
- Moulik, S. P., Rakshit, A. K., Pan, A., & Naskar, B. (2022). An overview of coacervates: The special disperse state of amphiphilic and polymeric materials in solution. *Colloids and Interfaces*, 6(3), 45. <https://doi.org/10.3390/colloids6030045>
- Nguyen, M.-H., Tran, T.-T., & Hadinoto, K. (2016). Controlling the burst release of amorphous drug-polysaccharide nanoparticle complex via crosslinking of the polysaccharide chains. *European Journal of Pharmaceutics and Biopharmaceutics*, 104, 156–163. <https://doi.org/10.1016/j.ejpb.2016.05.006>
- Nguyen, M. H., Yu, H., Kiew, T. Y., & Hadinoto, K. (2015). Cost-effective alternative to nano-encapsulation: Amorphous curcumin-chitosan nanoparticle complex exhibiting high payload and supersaturation generation. *European Journal of Pharmaceutics and Biopharmaceutics*, 96, 1–10. <https://doi.org/10.1016/j.ejpb.2015.07.007>
- Petrov, A. I., Antipov, A. A., & Sukhorukov, G. B. (2003). Base-Acid equilibria in polyelectrolyte systems: From weak polyelectrolytes to interpolyelectrolyte complexes and multilayered polyelectrolyte shells. *Macromolecules*, 36(26), 10079–10086. <https://doi.org/10.1021/ma034516p>
- Priyadarshini, K. I. (2009). Photophysics, photochemistry and photobiology of curcumin: Studies from organic solutions, bio-mimetics and living cells. *Journal of Photochemistry and Photobiology C: Photochemistry Reviews*, 10(2), 81–95. <https://doi.org/10.1016/j.jphotochem.2009.05.001>

- Rafiee, Z., Nejatian, M., Daeihamed, M., & Jafari, S. M. (2019). Application of curcumin-loaded nanocarriers for food, drug and cosmetic purposes. *Trends in Food Science & Technology*, 88, 445–458. <https://doi.org/10.1016/j.tifs.2019.04.017>
- Romero, D., Traxler, M. F., López, D., & Kolter, R. (2011). Antibiotics as signal molecules. *Chemical Reviews*, 111(9), 5492–5505. <https://doi.org/10.1021/cr2000509>
- Santos, M. B., de Carvalho, C. W. P., & Garcia-Rojas, E. E. (2018). Heteroprotein complex formation of bovine serum albumin and lysozyme: Structure and thermal stability. *Food Hydrocolloids*, 74, 267–274. <https://doi.org/10.1016/j.foodhyd.2017.08.016>
- Santos, M. B., Geraldo de Carvalho, M., & Garcia-Rojas, E. E. (2021). Carboxymethyl tara gum-lactoferrin complex coacervates as carriers for vitamin D3: Encapsulation and controlled release. *Food Hydrocolloids*, 112, Article 106347. <https://doi.org/10.1016/j.foodhyd.2020.106347>
- Shaddel, R., Hesari, J., Azadmard-Damirchi, S., Hamishehkar, H., Fathi-Achachlouei, B., & Huang, Q. (2018). Double emulsion followed by complex coacervation as a promising method for protection of black raspberry anthocyanins. *Food Hydrocolloids*, 77, 803–816. <https://doi.org/10.1016/j.foodhyd.2017.11.024>
- Shahgholian, N., & Rajabzadeh, G. (2016). Fabrication and characterization of curcumin-loaded albumin/gum Arabic coacervate. *Food Hydrocolloids*, 59, 17–25. <https://doi.org/10.1016/j.foodhyd.2015.11.031>
- de Silva, U. K., Brown, J. L., & Lapitsky, Y. (2018). Poly(allylamine)/tripolyphosphate coacervates enable high loading and multiple-month release of weakly amphiphilic anionic drugs: An in vitro study with ibuprofen. *RSC Advances*, 8(35), 19409–19419. <https://doi.org/10.1039/C8RA02588F>
- Sing, C. E., & Perry, S. L. (2020). Recent progress in the science of complex coacervation. *Soft Matter*, 16(12), 2885–2914. <https://doi.org/10.1039/D0SM00001A>
- Somu, P., & Paul, S. (2021). Surface conjugation of curcumin with self-assembled lysozyme nanoparticle enhanced its bioavailability and therapeutic efficacy in multiple cancer cells. *Journal of Molecular Liquids*, 338, Article 116623. <https://doi.org/10.1016/j.molliq.2021.116623>
- Su, C.-R., Huang, Y.-Y., Chen, Q.-H., Li, M.-F., Wang, H., Li, G.-Y., & Yuan, Y. (2021). A novel complex coacervate formed by gliadin and sodium alginate: Relationship to encapsulation and controlled release properties. *Lebensmittel-Wissenschaft & Technologie*, 139, Article 110591. <https://doi.org/10.1016/j.lwt.2020.110591>
- Thongkaew, C., Hinrichs, J., Gibis, M., & Weiss, J. (2015). Sequential modulation of pH and ionic strength in phase separated whey protein isolate – pectin dispersions: Effect on structural organization. *Food Hydrocolloids*, 47, 21–31. <https://doi.org/10.1016/j.foodhyd.2014.11.006>
- Tirrell, M. (2018). Polyelectrolyte complexes: Fluid or solid? *ACS Central Science*, 4(5), 532–533. <https://doi.org/10.1021/acscentsci.8b00284>
- Tønnesen, H. H., & Karlsen, J. (1985). Studies on curcumin and curcuminoids. *Zeitschrift für Lebensmittel-Untersuchung und -Forschung*, 180(5), 402–404. <https://doi.org/10.1007/BF01027775>
- Vieregg, J. R., Lueckheide, M., Marciel, A. B., Leon, L., Bologna, A. J., Rivera, J. R., & Tirrell, M. V. (2018). Oligonucleotide–Peptide complexes: Phase control by hybridization. *Journal of the American Chemical Society*, 140(5), 1632–1638. <https://doi.org/10.1021/jacs.7b03567>
- Wang, L., Liang, X., Chen, Y., Ding, B., Sun, W., Li, Z., & Luo, Y. (2021). Understanding the effects of carboxymethyl cellulose on the bioactivity of lysozyme at different mass ratios and thermal treatments. *Food Hydrocolloids*, 113, Article 106446. <https://doi.org/10.1016/j.foodhyd.2020.106446>
- Warnakulasuriya, S. N., & Nickerson, M. T. (2018). Review on plant protein-polysaccharide complex coacervation, and the functionality and applicability of formed complexes. *Journal of the Science of Food and Agriculture*, 98(15), 5559–5571. <https://doi.org/10.1002/jsfa.9228>
- Wu, T., Jiang, Q., Wu, D., Hu, Y., Chen, S., Ding, T., Ye, X., Liu, D., & Chen, J. (2019). What is new in lysozyme research and its application in food industry? A review. *Food Chemistry*, 274, 698–709. <https://doi.org/10.1016/j.foodchem.2018.09.017>
- Xu, W., Jin, W., Zhang, C., Li, Z., Lin, L., Huang, Q., Ye, S., & Li, B. (2014). Curcumin loaded and protective system based on complex of κ-carrageenan and lysozyme. *Food Research International*, 59, 61–66. <https://doi.org/10.1016/j.foodres.2014.01.059>
- Yang, D., Wang, Q., Chen, L., Liu, Y., Cao, R., Wu, H., Li, F., Ji, C., Cong, M., & Zhao, J. (2017). Molecular characterization and antibacterial activity of a phage-type lysozyme from the Manila clam, *Ruditapes philippinarum*. *Fish & Shellfish Immunology*, 65, 17–24. <https://doi.org/10.1016/j.fsi.2017.03.051>
- Yu, H., & Hadinoto, K. (2017). Impacts of dextran sulfate's chain length on the characteristics of its self-assembled colloidal complex formed with amphiphilic small-molecule drug. *International Journal of Biological Macromolecules*, 103, 493–500. <https://doi.org/10.1016/j.ijbiomac.2017.05.095>
- Zhang, Y., Batys, P., O'Neal, J. T., Li, F., Sannalokorpi, M., & Lutkenhaus, J. L. (2018). Molecular origin of the glass transition in polyelectrolyte assemblies. *ACS Central Science*, 4(5), 638–644. <https://doi.org/10.1021/acscentsci.8b00137>
- Zhang, W., Wang, R., Sun, Z., Zhu, X., Zhao, Q., Zhang, T., Cholewinski, A., Yang, F., Kuo, J., Zhao, B., Pinnaratip, R., Forooshani, P. K., & Lee, B. P. (2020). Catechol-functionalized hydrogels: Biomimetic design, adhesion mechanism, and biomedical applications. *Chemical Society Reviews*, 49(2), 433–464. <https://doi.org/10.1039/C9CS00285E>
- Zheng, J., Gao, Q., Ge, G., Sun, W., Van der Meeren, P., & Zhao, M. (2022). Encapsulation behavior of curcumin in heteroprotein complex coacervates and precipitates fabricated from β-conglycinin and lysozyme. *Food Hydrocolloids*, 133, Article 107964. <https://doi.org/10.1016/j.foodhyd.2022.107964>
- Zheng, J., Gao, Q., Ge, G., Wu, J., Tang, C., Zhao, M., & Sun, W. (2021). Heteroprotein complex coacervate based on β-conglycinin and lysozyme: Dynamic protein exchange, thermodynamic mechanism, and lysozyme activity. *Journal of Agricultural and Food Chemistry*, 69(28), 7948–7959. <https://doi.org/10.1021/acs.jafc.1c02204>
- Zheng, J., Gao, Q., Ge, G., Wu, J., Tang, C., Zhao, M., & Sun, W. (2022a). Dynamic equilibrium of β-conglycinin/lysozyme heteroprotein complex coacervates. *Food Hydrocolloids*, 124, Article 107339. <https://doi.org/10.1016/j.foodhyd.2021.107339>
- Zheng, J., Gao, Q., Ge, G., Wu, J., Tang, C., Zhao, M., & Sun, W. (2022b). Sodium chloride-programmed phase transition of β-conglycinin/lysozyme electrostatic complexes from amorphous precipitates to complex coacervates. *Food Hydrocolloids*, 124, Article 107247. <https://doi.org/10.1016/j.foodhyd.2021.107247>
- Zheng, B., & McClements, D. J. (2020). Formulation of more efficacious curcumin delivery systems using colloid science: Enhanced solubility, stability, and bioavailability. *Molecules*, 25(12), 2791. <https://doi.org/10.3390/molecules25122791>
- Zheng, J., Tang, C., & Sun, W. (2020). Heteroprotein complex coacervation: Focus on experimental strategies to investigate structure formation as a function of intrinsic and external physicochemical parameters for food applications. *Advances in Colloid and Interface Science*, 284, Article 102268. <https://doi.org/10.1016/j.cis.2020.102268>
- Zhou, L., Shi, H., Li, Z., & He, C. (2020). Recent advances in complex coacervation design from macromolecular assemblies and emerging applications. *Macromolecular Rapid Communications*, 41(21), Article 2000149. <https://doi.org/10.1002/marc.202000149>
- Zorofchian Moghadamtousi, S., Abdul Kadir, H., Hassandarvish, P., Tajik, H., Abubakar, S., & Zandi, K. (2014). A review on antibacterial, antiviral, and antifungal activity of curcumin. *BioMed Research International*, 1–12. <https://doi.org/10.1155/2014/186864>, 2014.